

Thermodynamics of light management in photovoltaic devicesUwe Rau,^{1,*} Ulrich W. Paetzold,¹ and Thomas Kirchartz^{1,2}¹*IEK5—Photovoltaik, Forschungszentrum Jülich GmbH, 52425 Jülich, Germany*²*Faculty of Engineering and CENIDE, University of Duisburg-Essen, Carl-Benz-Str. 199, 47057 Duisburg, Germany*

(Received 24 February 2014; revised manuscript received 29 May 2014; published 28 July 2014)

This paper elaborates a comprehensive theory of the thermodynamics of light management in solar cells explicitly considering imperfect light trapping, parasitic absorption and nonradiative recombination losses. A quantitative description of the entropic losses that reduce the open-circuit voltage and the energy conversion efficiency from the radiative limit towards realistic situations is presented. The theory embraces the fundamental limits for idealized solar cell devices given by the Yablonovitch limit and the Shockley-Queisser limit. We discriminate between reversible and irreversible entropic loss processes for four fundamental light management concepts: (i) conventional light trapping as an integral part of the device, (ii) geometric concentration of incident light, (iii) angular restriction of incoming and outgoing light, and (iv) light concentration by luminescent solar collectors. Based on this discrimination, a comprehensive discussion of the interplay between the loss processes and light management is presented. As part of this analysis, a new figure of merit for efficient light trapping in solar cells is introduced as well as an example of a deterministic light trapping concept which induces almost optimal light trapping.

DOI: [10.1103/PhysRevB.90.035211](https://doi.org/10.1103/PhysRevB.90.035211)

PACS number(s): 78.60.-b, 88.40.fc, 88.40.hj

I. INTRODUCTION

The necessity to contribute to a sustainable energy supply is the driving force behind the tremendous progress that has been made in developing more and more efficient solar cells and solar modules during the last decades. In recent years, this necessity has met the opportunity to use novel optical concepts for light management in solar cells [1–5]. Among the newly pursued approaches are the use of spectrally or directionally selective filters [6–9], plasmonics [2,4,10–15] nanophotonic light trapping [16,17], photonic crystals [18–23], whispering gallery modes [24,25], nanowire solar cells [26–30], and fluorescent solar concentrators [31–38]. While most concepts have been discussed theoretically for more than a decade [39–53], only recently advanced optical concepts that go beyond the classical concepts, like light trapping with rough interfaces [54] and geometrical concentration, have been realized experimentally. Among those concepts are the implementation of photonic crystals as intermediate reflectors [20] or directionally selective filters [6,55], the use of metal nanoparticles for light scattering embedded in the contact [11,56–60] or even in the active layer [61], as well the fabrication of solar cells made from wires with diameters from a few hundreds of nanometers [62,63] to a few microns [27], which are made from systems like Si [27,63,64], GaAs [26], or InP [62]. The light scattering in the wire array solar cells allow high absorptances relative to the volume of absorber material used. The importance of optical concepts for photovoltaics in general can be seen by the fact that the improvement of the optical properties of GaAs cells has recently led to new energy conversion efficiency records [65] for single-junction solar cells [66].

The aim of realizing devices with maximum efficiencies and optimum light trapping requires a careful examination

of the thermodynamic limits for both the solar cell energy conversion efficiency and the open-circuit voltage. Especially the question of how the open-circuit voltage depends on optical concepts like light trapping or angularly selective filters has been the subject of some debate recently [67,68]. The reference point for photovoltaic energy conversion is the Shockley-Queisser (SQ) theory [69] for the thermodynamic limit of the energy conversion efficiency of solar cells with a single band gap energy. In the SQ theory, the solar cell is described only by its band gap E_g and its temperature. The absorptance needed to calculate absorption and emission of the ideal solar cell in the SQ theory is a step function with zero absorption below and full absorption above E_g . This implies that the optical properties of the device and any concepts for light trapping are not considered in the original SQ theory.

The enhancement of light absorption in solar cells for geometrical optics is subject to another independent thermodynamic limitation. The Yablonovitch limit [40,41] describes the maximum path length enhancement (in the limit of weak absorptance) within the photovoltaic absorber, resulting from the optimum coupling of the density of optical states within the absorber to the density of optical states of the outside world.

In view of the fact that cutting-edge photovoltaic and photonic concepts come closer and closer to thermodynamic limitations, a theoretical approach is needed that not only describes limiting ideal cases but that also embraces the physics of real-world devices. Such a theory must be compatible with both thermodynamic limits (namely the SQ theory and the Yablonovitch limit) simultaneously but should be able to quantitatively describe departures from the ideal cases. This paper introduces a rigorous approach for the thermodynamic limit of the open-circuit voltage by explicitly taking into account the optics of the device. We derive an equation for the open-circuit voltage that shows how it is reduced relative to the SQ limit due to a series of entropic loss processes.

*Corresponding author: u.rau@fz-juelich.de

Using this equation, we explain how the open-circuit voltage is affected by the optics of the device in a series of cases, including light trapping, geometrical concentration, angular confinement, and the case of luminescent solar collectors. As part of this analysis, a new figure of merit used as a criterion for efficient light trapping in solar cells is introduced as well as an example of a concept for an almost optimal light trapping concept.

The paper is organized as follows: in Sec. II, existing thermodynamic limits for idealized solar cell devices, the SQ limit and the Yablonovitch limit, are summarized. In Sec. III, our theory on thermodynamics of light management is derived, starting with (Sec. III A) the recapitulation of fundamentals and (Sec. III B) the description of reversible and irreversible loss processes of the open-circuit voltage and power conversion efficiency, followed by (Sec. III C) the derivation of a universal term of the open-circuit voltage which discriminates additive thermodynamic loss processes and (Sec. III D) the application of this term to four fundamental light management concepts for photovoltaic energy conversion: (i) conventional light trapping, (ii) geometric concentration, (iii) angular restriction, and (iv) luminescent light collection. In Sec. IV, the influence of light trapping on the open-circuit voltage is discussed for realistic solar cells and different light management concepts. Therefore, we first present the derivation of a new figure of merit for efficient light trapping in solar cells with nonvanishing absorptance (Sec. IV A). The validity of this figure of merit is demonstrated in the following for partial Lambertian light trapping (Sec. IV B) and deterministic light trapping (Sec. IV C). The derived theory of the thermodynamics of light management is employed subsequently to describe the interplay between electrical properties and light management (Sec. IV D) and discriminate entropic loss processes that reduce the open-circuit voltage of realistic solar cells (Sec. IV E).

II. THERMODYNAMIC LIMITS

A. SQ limit

The SQ approach considers radiative recombination as the only limiting fundamental recombination loss mechanism in the framework of the principle of detailed balance. With this assumption, an ideal solar cell is also an ideal light-emitting diode (LED). The only variables in the SQ theory are the sun's temperature T_s , the temperature T_c of the cell, the band gap energy E_g , and "the solid angle subtended by the sun" [69].

The simplifications needed to arrive at such a simple picture are (i) defining the sun's radiation spectrum as that of a black body with temperature T_s , (ii) the assumption of a steplike absorption function for the solar cell, and (iii) the postulate of sufficient carrier mobility such that all generated electron-hole pairs contribute to the photo current. The line of arguments developed by SQ was extended in later work by relaxing these simplifications towards the cases of a terrestrial solar spectrum [70], specific material-related spectral absorptances [42], semiconductor materials with band tails [71] and band gap fluctuations [72], organic absorber materials [73,74], multijunction cells [75,76], intermediate band cells [77],

multiple exciton generation [78–80], fluorescent collectors [31,81], and finite mobilities [82].

B. Reciprocity relations

Another branch of generalizations to the SQ theory concerns the inclusion of nonradiative recombination. In 1967, Ross [83] derived an equation for the attainable "potential difference μ caused by a radiation field in a photochemical system." An equivalent equation was derived also by Smestad and Ries [84] and in Ref. [85] using somewhat different approaches and notations. In the notation of Ref. [85], this relation reads

$$V_{\text{OC}} = V_{\text{OC}}^{\text{rad}} + \frac{kT_c}{q} \log(Q_e^{\text{LED}}), \quad (1)$$

where $V_{\text{OC}}^{\text{rad}}$ is the open-circuit voltage that would be attained if radiative losses, i.e. losses by photon emission from the solar cell, were the only loss mechanism. The quantity Q_e^{LED} is the external LED quantum efficiency of the device defined via

$$Q_e^{\text{LED}} = \frac{J_0^{\text{rad}}}{J_0^{\text{rad}} + J_0^{\text{nrad}}}. \quad (2)$$

Here, we distinguish the saturation current J_0^{rad} that leads to emission of one photon per injected electron from the saturation current J_0^{nrad} that does not lead to photon emission. The transition to the radiative limit is given by $Q_e^{\text{LED}} = 1$ (ideal LED) and, consequently $V_{\text{OC}} = V_{\text{OC}}^{\text{rad}}$.

For thermal radiation and time symmetric systems, Kirchhoff's law [86] is valid equating the absorptance of a body and its emissivity. Thus, together with the knowledge of the body's temperature and Planck's law [87], it is possible to calculate the thermal emission if the absorptance is known. This concept is the basis of the SQ limit; however, only in 1967, it was formally shown by Ross [83] and later derived in more detail by Würfel [88,89] that this principle can be extended to emission in terms of a chemical potential by considering equilibrium with a radiation field. However, the relation between absorption and emission in a semiconductor is only valid as long as the quasi-Fermi level splitting is constant over the whole volume of the absorber. To combine the optical reciprocity with transport, an equation connecting the external quantum efficiency Q_e^{PV} of a solar cell and the electroluminescence emission ϕ_{em} was derived in literature via [85]

$$\delta\phi_{\text{em}}(E) = Q_e^{\text{PV}}(E)\phi_{\text{bb}}(E) \left[\exp\left(\frac{qV}{kT_c}\right) - 1 \right]. \quad (3)$$

Both Eqs. (1) and (3) are reciprocity relations because they compare the same device in different operation modes. Equation (1) compares the open-circuit situation under illumination with the situation of applied forward bias in the dark, while Eq. (3) compares the short circuit under illumination, again with applied forward bias in the dark. Both Eqs. (1) and (3) have been extensively tested in a series of different material systems [90–97]. Usually, the agreement is very good within the experimental error. Deviations arise in systems where the original derivation is not applicable, as for instance disordered pin solar cells like amorphous or microcrystalline Si [98]. It shall be noted that time symmetry is assumed for Kirchhoff's law, which is fundamental to the reviewed theories in this

section. Only very recently have the consequences of breaking the time symmetry on photovoltaic systems been investigated [99].

C. Yablonovitch limit

The thermodynamic limit for light trapping is expressed as the maximum path length enhancement. Coupling of all optical modes inside the absorber to the outside world leads to an effective path length

$$l_{\text{eff}} = \langle l \rangle = 4n^2w. \quad (4a)$$

Here, n is the refractive index of the material, and w is the thickness of the absorber. Equation (4) means that the weakly absorbed light will travel on average a path that is $4n^2$ larger than the cell thickness within the solar cell. To reach an average path length enhancement of $4n^2$, the light has to be reflected multiple times at front and back contact, which means that parasitic absorption in the front or back contact layers will have a large influence on the experimentally achievable path length enhancement [6,66]. For weakly absorbed light, the absorptance is simply given by

$$A(E) = 4n^2w\alpha(E). \quad (4b)$$

For ergodic systems, where all photon states are occupied equally, the Yablonovitch limit was derived first in 1982. Minano and Luque provided an extension on the implications of this limit to arbitrary photovoltaic devices [44,100,101].

Importantly, Eqs. (4a) and (4b) are valid for an isotropic absorptance, i.e. if the angle under which the light beam impinges on the solar cell does not affect the average path length and therefore the absorptance. Angular selectivity of the solar cell allows overcoming the limit presented in Eq. (4a) since the path length can be enhanced for some angles of incidence if it is reduced for others [100,101]. In general, the absorption $A(E, \theta, \varphi)$ integrated over the angles θ and φ reads

$$4\pi n^2\alpha(E)w \geq \int_0^{2\pi} \int_0^{\pi/2} A(E, \theta, \varphi) \sin(\theta) \cos(\theta) d\varphi d\theta, \quad (5)$$

where α is the absorption coefficient of the material (see Supplemental Material [102]). Thus, reducing the absorptance $A(E, \theta, \varphi)$ for certain angles could be used to increase the path length for some angles much beyond the limit given by Eq. (4a). To provide an example, if we define the étendue of the incoming beam as $\varepsilon_{\text{in}} = \pi S_{\text{in}} \sin^2(\theta_{\text{in}})$, where S_{in} is the area from which light is collected to fall onto the solar cell (i.e. either the area of the solar cell or, in the case of geometrical concentration, the area of the lens used for concentration), and θ_{in} is the angle relative to the surface normal (see Fig. 1), the effective path length enhancement becomes

$$l_{\text{eff}} = \langle l \rangle = 4n^2w \frac{S_{\text{in}}\pi}{\varepsilon_{\text{in}}} = \frac{4n^2w}{\sin^2(\theta_{\text{in}})}. \quad (6)$$

This enhancement in path length is valid for the beams that impinge on the solar cell within the angle θ_{in} . For other angles, light trapping would have to be worse such that Eq. (5) is not violated. In addition, Eq. (6) implies that light trapping by angularly selective absorption would require the solar cell to be tracked such that the sun always impinges on the cell under the

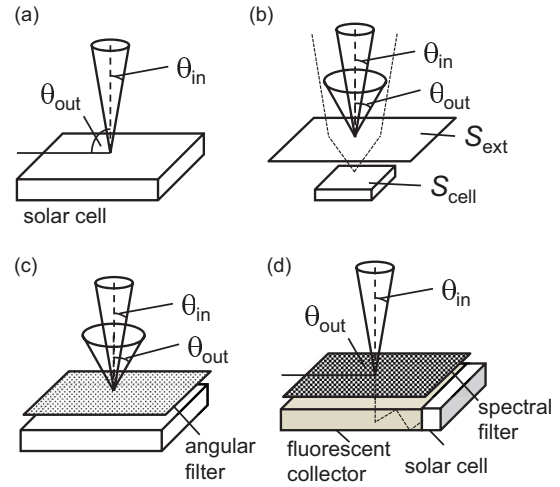


FIG. 1. (Color online) Schematic illustrations of four fundamental light-management concepts: (a) conventional light trapping as an integral part of the device, (b) geometric concentration of incident light, (c) angular restriction of incoming and outgoing light, and (d) luminescent solar collectors. The acceptance angle (θ_{in}) and emission angle (θ_{out}) of the light cones of incident and emitted light are shown.

same angle of incidence and benefits from the enhanced light trapping. The benefits of angular selectivity for photovoltaics have been first identified by Green [103] and described more quantitatively in the light-trapping context by Campbell and Green [104].

It is important to note that improving the absorptance by light trapping also improves the emissivity according to Kirchhoff's law. This is still valid in the case of luminescence emitted from solar cells or light-emitting diodes. This means that improved light outcoupling and improved light incoupling or light trapping are identical at least as long as the absorptance is isotropic. Even in the radiative limit, it is therefore possible to increase the energy conversion efficiency of a solar cell by increasing the loss due to radiative recombination. This is possible if the increase in energy conversion efficiency due to a higher photocurrent (improved by light trapping) outweighs the loss due to increased emission by improved light outcoupling.

One fundamental limitation of the Yablonovitch limit is the limitation of light propagation to geometrical optics. This limitation is only valid if the thickness of the absorber layer is much larger than the wavelength of the incident light and geometrical parameters, such as grating periods of light-trapping schemes, are of dimensions of many wavelengths. In particular, for thin-film solar cells, these assumptions are not valid. In a recent work, Yu *et al.* [17,49] have shown that the generalized Yablonovitch limit for the case of vanishing absorptance [Eq. (6)] remains valid for thicknesses and grating periods in the order of the wavelength of visible light. Possible ways presented in recent literature which in theory would allow one to exceed the generalized form of the Yablonovitch limit [Eq. (6)] are the concept of tunneling evanescent waves [16] or the concept of subwavelength-scale electric-field confinement [16,17].

III. THEORY

A. Recapitulation of fundamentals

The fundamental textbook relation of the energy-conversion efficiency η of a solar cell reads

$$\eta = \frac{J_{\text{mpp}} V_{\text{mpp}}}{P_{\text{in}}} = \frac{FF J_{\text{SC}} V_{\text{OC}}}{P_{\text{in}}}, \quad (7)$$

where J_{SC} is the short-circuit current density, V_{OC} is the open-circuit voltage, V_{mpp} is the voltage at the maximum power point, J_{mpp} is the current density at the maximum power point, P_{in} is the incident solar energy current, and FF is the fill factor. The V_{OC} of a solar cell is given by [43]

$$V_{\text{OC}} = \frac{kT_c}{q} \ln \left\{ \frac{J_{\text{SC}}}{J_0} + 1 \right\} \approx \frac{kT_c}{q} \ln \left\{ \frac{J_{\text{SC}}}{J_0} \right\}, \quad (8)$$

where k denotes the Boltzmann constant, T_c the absolute temperature of the solar cell, q the elementary charge, and J_0 the saturation current of the solar cell.

With

$$J_0 = J_0^{\text{rad}} + J_0^{\text{non-rad}} \quad (9)$$

and Eq. (2), we can rewrite Eq. (8) arriving at

$$\begin{aligned} qV_{\text{OC}} &= kT_c \ln \left\{ \frac{J_{\text{SC}}}{J_0^{\text{rad}}} \right\} + kT_c \ln \left\{ Q_e^{\text{LED}} \right\} \\ &= qV_{\text{OC}}^{\text{rad}} + kT_c \ln \left\{ Q_e^{\text{LED}} \right\}. \end{aligned} \quad (10)$$

The second term contains all entropic loss processes that are connected with nonradiative recombination and parasitic absorption of photons within the system. It is important to mention that $V_{\text{OC}}^{\text{rad}}$ as used in Eq. (10) has a significant dependence on the optical and electrical properties of the solar cell and is only of limited use as a reference value as we will see in the following.

Because of the principle of detailed balance, the emission and absorption properties of a solar cell are interlinked, and we have for the radiative (emission) saturation current

$$J_0^{\text{rad}} = q\varepsilon_{\text{out}} \int A(E)\phi_{\text{bb}}(E)dE, \quad (11)$$

where ε_{out} is the étendue of the emitted light and

$$\phi_{\text{bb}} = \frac{2E^2}{h^3c^2} \exp\left(-\frac{E}{kT_c}\right) \quad (12)$$

is the black body radiation flux at the cell's temperature per unit area and unit spherical angle with h being Planck's constant and c the vacuum speed of light. Analogously, the short-circuit current is defined by

$$J_{\text{SC}} = q\varepsilon_{\text{in}} \int A(E)\phi_{\text{sun}}(E)dE, \quad (13)$$

with ε_{in} as the étendue of the incoming light and the photon flux $\phi_{\text{sun}}(E)$ of the sun. Note that, for simplicity, we have assumed that the absorptance $A(E)$ is independent of the angle of incidence and that all photons that are absorbed by the photovoltaic absorber material contribute to J_{SC} , i.e. the external photovoltaic quantum efficiency $Q_e^{\text{PV}}(E)$ equals $A(E)$, i.e. the carrier collection efficiency within the photovoltaic absorber is unity.

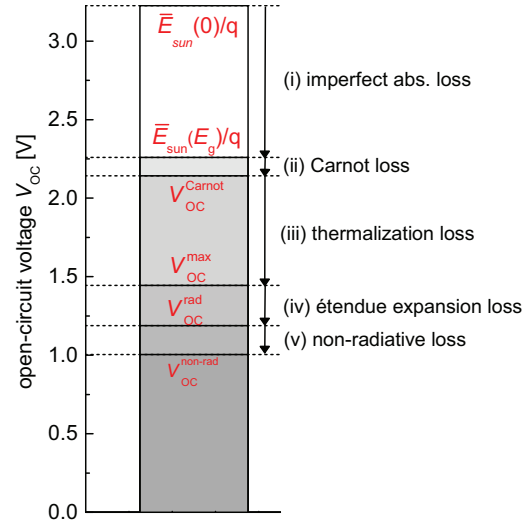


FIG. 2. (Color online) Thermodynamic limitations of the open-circuit voltage V_{OC} of a single solar cell (idealized semiconductor with $E_g = 1.38$ eV, step-function-like absorptance and $Q_e^{\text{LED}}(E) = 10^{-3}$) limiting also the overall power conversion efficiency since $\eta \leq J_{\text{SC}} V_{\text{OC}} / P_{\text{in}}$.

B. Thermodynamic limitations of the energy conversion efficiency

The thermodynamic limitations of the energy conversion efficiency of a solar cell are described in literature making use of $\eta < \eta_{\text{limit}} = J_{\text{SC}} \cdot V_{\text{OC}} / P_{\text{in}}$ [see Eq. (7)] and an idealized semiconductor material [$A(E) = 1$ for $E \geq E_g$]. In view of this upper bound η_{limit} , which neglects the effect of the fill factor of the solar cell, the limitation of η is described by the imperfect absorption of incident light which limits J_{SC} and four additive entropic loss processes that reduce V_{OC} . In the following, these limitations are recapitulated and illustrated in Fig. 2 for an idealized semiconductor [$E_g = 1.38$ eV and $Q_e^{\text{LED}}(E) = 10^{-3}$].

(i) *Imperfect absorption loss*: For a single junction solar cell, the use of the solar energy current is limited by the band gap energy. The maximum accessible short-circuit current density $J_{\text{SC}}^{\text{max}}$ is given for perfect absorption of light of energy above E_g and no absorption of light of energy below E_g . In order to obtain a properly defined thermodynamic limitation for the open-circuit voltage of a single junction solar cell, we refer in the following to the average energy of photons (above the band gap energy E_g):

$$\bar{E}_{\text{sun}}(E_g) = \frac{\int_{E_g}^{\infty} E \phi_{\text{sun}}(E) dE}{\int_{E_g}^{\infty} \phi_{\text{sun}}(E) dE}. \quad (14)$$

Thus, the energy loss due to nonabsorption amounts to $\bar{E}_{\text{sun}}(0) - \bar{E}_{\text{sun}}(E_g)$, where $\bar{E}_{\text{sun}}(0) = \int_0^{\infty} E \phi_{\text{sun}} dE / \int_{E_g}^{\infty} \phi_{\text{sun}} dE$, i.e. $\bar{E}_{\text{sun}}(0)$ is equal to the total power density in the solar spectrum divided by $J_{\text{SC}}^{\text{max}}$.

(ii) *Carnot loss*. From the thermodynamic perspective, a solar cell can be viewed as a heat engine which generates work while heat flows from the hot reservoir of the sun ($T_s = 5800$ K) to the cold reservoir of the solar cell device with its surrounding atmosphere ($T_c = 300$ K) [43,105]. To understand reversible

entropy generation, we first consider the open-circuit voltage of a monochromatic solar cell [106]. Such a device interacts with the sun only at a single wavelength E_{mo} and, therefore, may be considered as a two-level system [107]. In the radiative limit and under full concentration, the device exclusively interacts with the sun, and there is no thermalization. Thus, the open-circuit voltage $qV_{\text{OC}}^{\text{mo}} = E_{\text{mo}}(1 - T_c/T_s)$ [107] is a true Carnot value that describes the limiting efficiency of the conversion of a single photon into electrical energy when the device is kept under open-circuit voltage. This process is reversible since injection of an electron-hole pair at $V_{\text{OC}}^{\text{mo}}$ sends a photon of energy E_{mo} to the sun such that no energy is lost in the cycle. Considering now the average energy turnover by photon (i.e. $V_{\text{OC}}^{\text{mo}}$) for an infinite number of monochromatic two state solar cells with $E_{\text{mo}} \geq E_g$, we obtain the Carnot limit for the open-circuit voltage

$$V_{\text{OC}}^{\text{Carnot}} = \frac{\bar{E}_{\text{sun}}(E_g)}{q} \left(1 - \frac{T_c}{T_s}\right). \quad (15)$$

This value corresponds to the maximum open-circuit voltage that can be obtained by a reversible process that makes use of all solar photons with energy larger than the band gap energy E_g .

(iii) *Thermalization loss*: In a single junction solar cell, the charge carriers which are excited beyond the band gap thermalize to the energy levels close to E_g . As described by the SQ theory, this irreversible loss process leads to a decrease of V_{OC} below the Carnot limit. In the Boltzmann approximation, the corresponding open-circuit voltage was derived before, e.g. Ruppel and Würfel [108], and in a thermodynamic context by Markvart [109] and by Hirst and Ekens-Daukes [110] as

$$V_{\text{OC}}^{\text{max}} = \frac{E_g}{q} \left(1 - \frac{T_c}{T_s}\right) + \frac{kT_c}{q} \ln \left\{ \frac{T_s [2(kT_s)^2 + 2kT_s E_g + E_g^2]}{T_c [2(kT_c)^2 + 2kT_c E_g + E_g^2]} \right\} \\ \approx \frac{E_g}{q} \left(1 - \frac{T_c}{T_s}\right) + \frac{kT_c}{q} \ln \left(\frac{T_s}{T_c}\right). \quad (16)$$

It must be emphasized that the first term on the right side of Eq. (16) is not identical to the previously introduced $V_{\text{OC}}^{\text{Carnot}}$ [see Eq. (15)] and that its Carnot-like form does not imply reversible entropy generation. The second term represents the increase in energy of charge carriers at the band edge due to their thermal energy. The frequently used term in the second line of Eq. (16) is a good approximation for band gaps of typical solar cell materials [109] and gets worse towards smaller band gaps when kT_s is not negligibly small relative to E_g .

(iv) *Étendue expansion loss*: An additional thermodynamic loss is associated with the increase in solid angle between the photons emitted from the solar cell and the incident photons from the sun. If the étendue of the emitted photons (ε_{out}) from the solar cell is larger than the small étendue of the incident photons of the sun (ε_{in}), entropy will be produced since the directional order of the photons is decreased. This irreversible thermodynamic loss process is expressed by [76,110,111]

$$V_{\text{OC}}^{\text{étendue}} = V_{\text{OC}}^{\text{max}} + \frac{kT_c}{q} \ln \left(\frac{\varepsilon_{\text{in}}}{\varepsilon_{\text{out}}}\right). \quad (17)$$

It shall be noted that, in the case of full concentration, the solid angle of the emitted photons and incident photons are equal,

and the thermodynamic emission loss vanishes. Furthermore, the expression in Eq. (17) is equal to $V_{\text{OC}}^{\text{rad}}$.

(v) *Nonradiative loss*: Finally, nonradiative recombination losses or parasitic optical losses in the solar cell induce thermalization of charge carriers in the device which produces thermal losses, i.e. entropy. The contribution of this irreversible thermodynamic loss process to the thermodynamic limitation is described by

$$V_{\text{OC}}^{\text{nonrad}} = V_{\text{OC}}^{\text{étendue}} + \frac{kT_c}{q} \ln \{Q_e^{\text{LED}}\}. \quad (18)$$

C. Entropy generation at open circuit

Beyond the above-described thermodynamic limitations of η and V_{OC} , rigorous terms of the entropic loss processes associated with light trapping, parasitic absorption, and nonradiative recombination will be derived in the following. The rigorous derivation allows for a general description of the limitations in realistic solar cells with $FF < 1$. The treatment explicitly implies imperfect absorption of incident light close to E_g which requires light-trapping concepts. We start from the equation

$$qV_{\text{OC}} = kT_c \ln \left\{ \frac{\varepsilon_{\text{in}} \int A(E) \phi_{\text{sun}}(E) dE}{\varepsilon_{\text{out}} \int A(E) \phi_{\text{bb}}(E) dE} \right\} + kT_c \ln \{Q_e^{\text{LED}}\}, \quad (19)$$

which is derived by inserting Eq. (11) and Eq. (13) into Eq. (10). In the next step, we introduce the radiative and nonradiative recombination rates R_{rad} and R_{nrad} . For radiative recombination, we further distinguish between recombination that leads to emission of a photon with a probability p_e , reabsorption of the photon in the photovoltaic absorber with probability p_r , and parasitic absorption with probability p_a . With these definitions, the overall saturation current is given by

$$J_0 = qS_{\text{cell}}w [R_{\text{nrad}} + (1 - p_r)R_{\text{rad}}], \quad (20)$$

where w and S_{cell} denote the thickness and the surface area of the cell. To derive Eq. (20), we have to assume that the recombination rates are independent of the position in the absorber. Note that this assumption is consistent with our earlier assumption $Q_c^{\text{pn}}(E) = A(E)$ because, by Donolato's reciprocity relation [112], a carrier collection efficiency of unity in the illuminated case implies flat quasi-Fermi levels in the dark situation under applied voltage bias. Thus, we have

$$qV_{\text{OC}} = kT_c \ln \left\{ \frac{\varepsilon_{\text{in}} \int A(E) \phi_{\text{sun}}(E) dE}{\varepsilon_{\text{out}} \int A(E) \phi_{\text{bb}}(E) dE} \right\} \\ + kT_c \ln \left\{ \frac{\varepsilon_{\text{out}} \int A(E) \phi_{\text{bb}}(E) dE}{S_{\text{cell}}w [R_{\text{nrad}} + (1 - p_r)R_{\text{rad}}]} \right\}, \quad (21)$$

taking into account that reabsorption (photon recycling) is not a loss mechanism. In the next step, we define the internal luminescence quantum efficiency via

$$Q_i^{\text{lum}} = \frac{R_{\text{rad}}}{R_{\text{rad}} + R_{\text{nrad}}}. \quad (22)$$

This step is important because, with Q_i^{lum} , we are able to refer to a pure bulk property of the photovoltaic absorber material. Analogously, the radiative recombination rate is a

property that is connected to the absorption coefficient of the absorber material via the van Roosbroeck-Shockley equation [113] according to

$$R_{\text{rad}} = \int \alpha(E) 4\pi n^2 \phi_{\text{bb}}(E) dE. \quad (23)$$

With Eqs. (22) and (23), we finally arrive at an equation that contains four additive terms that describe the four entropic loss processes

$$\begin{aligned} qV_{\text{OC}} = & kT_c \ln \left\{ \frac{\int A(E) \phi_{\text{sun}}(E) dE}{\int A(E) \phi_{\text{bb}}(E) dE} \right\} + kT_c \ln \left\{ \frac{\varepsilon_{\text{in}}}{\varepsilon_{\text{out}}} \right\} \\ & + kT_c \ln \left\{ \frac{\varepsilon_{\text{out}} \int A(E) \phi_{\text{bb}}(E) dE}{4n^2 \pi S_{\text{cell}} w \int \alpha(E) \phi_{\text{bb}}(E) dE} \right\} \\ & + kT_c \ln \left\{ \frac{Q_i^{\text{lum}}}{(1 - Q_i^{\text{lum}}) + (1 - p_r) Q_i^{\text{lum}}} \right\}. \quad (24) \end{aligned}$$

The first term of Eq. (24) accounts for the different temperatures of the incoming and the outgoing photons. It

corresponds to $V_{\text{OC}}^{\text{max}}$ introduced in Eq. (16) for idealized solar cells and considers the imperfect absorption photons and the thermalization losses. The second term describes the étendue expansion between the incident and emitted photons, which was introduced in Eq. (17) for an idealized solar cell [109,111]. These two terms together define $V_{\text{OC}}^{\text{rad}}$ in Eq. (1). Term 3 represents the ratio between the outgoing photon flux and the integral radiative recombination in the cell. This ratio corresponds to the emission probability

$$p_e = \frac{\varepsilon_{\text{out}} \int A(E) \phi_{\text{bb}}(E) dE}{4n^2 \pi S_{\text{cell}} w \int \alpha(E) \phi_{\text{bb}}(E) dE}. \quad (25)$$

Because every photon generated by radiative recombination will either be emitted (with probability p_e), reabsorbed (p_r), or parasitically absorbed (p_a), $p_e + p_a + p_r = 1$ holds for the sum of the three probabilities. Therefore, we may write Eq. (24) alternatively as

$$\begin{aligned} qV_{\text{OC}} = & kT_c \ln \left\{ \frac{\int A(E) \phi_{\text{sun}}(E) dE}{\int A(E) \phi_{\text{bb}}(E) dE} \right\} + kT_c \ln \left\{ \frac{\varepsilon_{\text{in}}}{\varepsilon_{\text{out}}} \right\} \\ & + kT_c \ln \left\{ \frac{p_e}{p_e + p_a} \right\} + kT_c \ln \left\{ \frac{(p_e + p_a) Q_i^{\text{lum}}}{(1 - Q_i^{\text{lum}}) + (p_e + p_a) Q_i^{\text{lum}}} \right\}. \quad (26) \end{aligned}$$

This alternative form enables one to discriminate term by term the entropic loss processes that reduce the open-circuit voltage due to (1) photon cooling, (2) étendue expansion, (3) parasitic absorption, and (4) nonradiative recombination in the volume of the photovoltaic absorber.

It is important to notice that, in the general case, none of those four entropic loss processes is independent from the others. For instance, the numerator of term 3 of Eq. (24) cancels out with the denominators in terms 1 and 2, or the emission probability p_e shows up in term 3 and 4. Thus, the simple additive form of Eqs. (24) or (26) has to be handled with care.

In order to organize Eq. (24) in a form that only contains independent terms, we have to give up the additive form of Eqs. (24) or (26). Instead, we write

$$qV_{\text{OC}} = kT_c \ln \left(\frac{Q_i^{\text{lum}} \varepsilon_{\text{in}} \int A \phi_{\text{sun}} dE}{Q_i^{\text{lum}} \varepsilon_{\text{out}} \int A \phi_{\text{bb}} dE + (1 - Q_i^{\text{lum}}) \varepsilon_{\text{cell}} 4n^2 w \int \alpha \phi_{\text{bb}} dE + Q_i^{\text{lum}} p_a \pi S_{\text{cell}} 4n^2 w \int \alpha \phi_{\text{bb}} dE} \right). \quad (27)$$

For simplicity, we introduce for the following current densities (per unit étendue) for the sun's radiation:

$$i_{\text{sun}} = q \int A \phi_{\text{sun}} dE, \quad (28)$$

for the photons emitted by the solar cell

$$i_{\text{rad}}^{\text{em}} = q \int A \phi_{\text{bb}} dE, \quad (29)$$

and for the total radiative recombination in the volume of the absorber

$$i_{\text{rad}}^{\text{vol}} = qw 4n^2 \int \alpha \phi_{\text{bb}} dE. \quad (30)$$

With these definitions, we arrive at the general equation

$$qV_{\text{OC}} = kT_c \ln \left[\frac{Q_i^{\text{lum}} \varepsilon_{\text{in}} i_{\text{sun}}}{(1 - Q_i^{\text{lum}}) \pi S_{\text{cell}} i_{\text{rad}}^{\text{vol}} + Q_i^{\text{lum}} (p_a \pi S_{\text{cell}} i_{\text{rad}}^{\text{vol}} + \varepsilon_{\text{out}} i_{\text{rad}}^{\text{em}})} \right], \quad (31)$$

which, in contrast to Eqs. (24) and (26), contains no duplicate terms.

D. Application to different photovoltaic systems

In the following, we use Eq. (31) to analyze different types of solar cell systems, normal solar cells, geometrical concentrators, cells with angular selective filters, and fluorescent concentrators as illustrated in Figs. 1(a)–1(d). We first analyze the influence of nonradiative recombination in the bulk of the solar cell embedded into the four different systems. Since the incoming and outgoing light is considered outside of the system (i.e. in air or vacuum with a dielectric constant $n = 1$), the étendues read $\varepsilon_{\text{in/out}} = \pi S_{\text{in/out}} \sin^2(\theta_{\text{in/out}})$, and we have for the external areas of the systems $S_{\text{in}} = S_{\text{out}} = S_{\text{ext}}$ for all systems in Fig. 1. With this, Eq. (31) transforms into

$$qV_{\text{OC}} = kT_c \ln \left[\frac{Q_i^{\text{lum}} i_{\text{sun}} S_{\text{ext}} \sin^2(\theta_{\text{sun}})}{(1 - Q_i^{\text{lum}}) S_{\text{cell}} i_{\text{rad}}^{\text{vol}} + Q_i^{\text{lum}} S_{\text{cell}} i_{\text{rad}}^{\text{vol}} p_a + Q_i^{\text{lum}} S_{\text{ext}} \sin^2(\theta_{\text{out}}) i_{\text{rad}}^{\text{em}}} \right]. \quad (32)$$

For the first case, the normal nonconcentrating solar cells, we have $S_{\text{ext}} = S_{\text{cell}}$, $\theta_{\text{out}} = \pi/2$, and therefore we have

$$qV_{\text{OC}} = kT_c \ln \left[\frac{Q_i^{\text{lum}} i_{\text{sun}} \sin^2(\theta_{\text{sun}})}{(1 - Q_i^{\text{lum}}) i_{\text{rad}}^{\text{vol}} + Q_i^{\text{lum}} i_{\text{rad}}^{\text{vol}} p_a + Q_i^{\text{lum}} i_{\text{rad}}^{\text{em}}} \right]. \quad (33)$$

The second case concerns a solar cell with geometric concentration. Here, we define the geometric concentration factor via $c_{\text{geo}} := S_{\text{ext}}/S_{\text{cell}}$. Because of the conservation of étendue, we have $\sin^2(\theta_{\text{out}}) = 1/c_{\text{geo}}$ and, thus,

$$qV_{\text{OC}} = kT_c \ln \left[\frac{c_{\text{geo}} Q_i^{\text{lum}} i_{\text{sun}} \sin^2(\theta_{\text{sun}})}{(1 - Q_i^{\text{lum}}) i_{\text{rad}}^{\text{vol}} + Q_i^{\text{lum}} i_{\text{rad}}^{\text{vol}} p_a + Q_i^{\text{lum}} i_{\text{rad}}^{\text{em}}} \right]. \quad (34)$$

As a third case, we have a solar cell with angular restriction to the incoming and outgoing light. Here, we define a concentration factor $c_{\text{ang}} := 1/\sin^2(\theta_{\text{out}})$, whereas for the surface areas, we have $S_{\text{out}} = S_{\text{cell}}$, i.e. $c_{\text{geo}} = 1$. Thus, Eq. (32) turns into

$$qV_{\text{OC}} = kT_c \ln \left[\frac{c_{\text{ang}} Q_i^{\text{lum}} i_{\text{sun}} \sin^2(\theta_{\text{sun}})}{c_{\text{ang}} (1 - Q_i^{\text{lum}}) i_{\text{rad}}^{\text{vol}} + c_{\text{ang}} Q_i^{\text{lum}} i_{\text{rad}}^{\text{vol}} p_a + Q_i^{\text{lum}} i_{\text{rad}}^{\text{em}}} \right]. \quad (35)$$

Finally, we consider a luminescent collector [114]. In a fluorescent collector, the sunlight is first absorbed by a fluorescent dye and subsequently reemitted at lower photon energies. The reemitted light is randomized and, due to total internal reflection, guided to a solar cell. The collection of photons can be greatly enhanced by a band-stop filter that is reflecting the photon energies of the light emitted by the dye [31]. The energy shift by the dye relaxes the requirement for étendue conservation [81] of conventional concentrators. Furthermore, the absorptance A^C of the collector is now defined by the dye and by the filter such that we have to redefine the current densities i_{sun} and $i_{\text{rad}}^{\text{em}}$ [Eqs. (28) and (29)] by

$$i_{\text{sun}}^C = q \int A^C \phi_{\text{sun}} dE, \quad (36)$$

and

$$i_{\text{rad}}^{\text{em}C} = q \int A^C \phi_{\text{bb}} dE, \quad (37)$$

respectively, whereas the recombination current density due to bulk recombination, Eq. (30), remains unchanged. To warrant perfect photon collection, we must assume that the chemical potential μ of photons is uniform within the collector [81] and that the collector is equipped with the band-stop filter [31,115] as sketched in Fig. 1(d). With this assumption, the entire photovoltaic action of the system is described analytically in terms of the étendues of photons entering and leaving the collector from/into the ambient and from/into the solar cell [81].

Starting with Eq. (36), we introduce nonradiative recombination in the solar cell in the same way as above and arrive at the same result, i.e. Eqs. (24) and (36) just with A replaced

by A^C . For a fluorescent concentrator, we have, again, a geometric concentration factor $c_{\text{geo}} := S_{\text{ext}}/S_{\text{cell}}$, but unlike in the geometric concentrator, we have for the angular concentration $c_{\text{ang}} = 1/\sin^2(\theta_{\text{out}}) = 1$. Therefore, Eq. (32) reads

$$qV_{\text{OC}} = kT_c \ln \left[\frac{c_{\text{geo}} Q_i^{\text{lum}} i_{\text{sun}}^* \sin^2(\theta_{\text{sun}})}{(1 - Q_i^{\text{lum}}) i_{\text{rad}}^{\text{vol}} + Q_i^{\text{lum}} i_{\text{rad}}^{\text{vol}} p_a + c_{\text{geo}} Q_i^{\text{lum}} i_{\text{rad}}^{\text{em}*}} \right]. \quad (38)$$

It shall be noted that the derivation of Eq. (32) by simply replacing A by A^C is only valid as long as photon collection within the fluorescent concentrator is warranted [115], which is the case for the parameters used in the calculations below.

Figure 3(a) compares the results for all four cases discussed above (assuming no parasitic absorption, i.e. $p_a = 0$, and a ratio $i_{\text{rad}}^{\text{em}}/i_{\text{rad}}^{\text{vol}} = 0.5$ for all curves). Firstly, the figure shows the open-circuit voltage calculated from Eq. (31) for a normal solar cell ($c_{\text{geo}} = c_{\text{ang}} = 1$) as a function of the internal luminescence efficiency Q_i^{lum} . Note that the V_{OC} axis in Fig. 3(a) is offset by the radiative limit $V_{\text{OC}}^{\text{rad},1}$ of this solar cell without concentration. Also shown are the V_{OC} curves calculated for geometric concentrations $c_{\text{geo}} = c_{\text{ang}} = 10$ and 100 from Eq. (34). These curves are simply shifted by an amount $kT_c \ln(c_{\text{geo}})$ with respect to V_{OC} of the cell without concentration.

To calculate V_{OC} for the case of angular restriction, we use Eq. (35) with $c_{\text{ang}} = 100$. The corresponding curve in Fig. 3(a) has a radiative limit that is larger by an amount

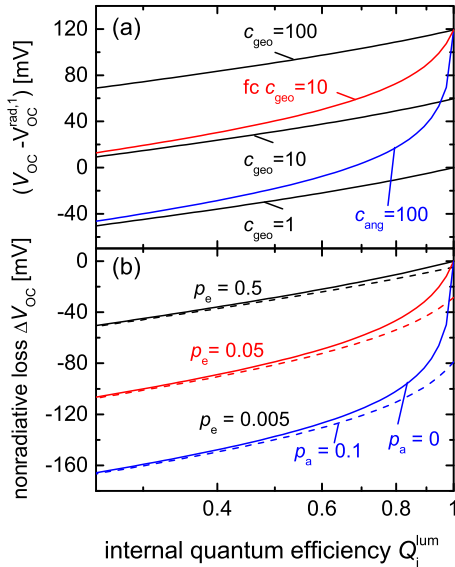


FIG. 3. (Color online) (a) The enhancement of the open-circuit voltage V_{OC} relative to the open-circuit voltage in the radiative limit $V_{OC}^{rad,1}$ is shown as a function of the internal luminescence quantum efficiency Q_i^{lum} for the four fundamental light-management concepts: conventional light trapping ($c_{geo} = c_{ang} = 1$), geometric concentration of incident light ($c_{geo} > 1, c_{ang} = 1$), angular restriction of incoming and outgoing light ($c_{geo} = 1, c_{ang} > 1$), and luminescent solar collectors ($fc\ c_{geo} > 1$). (b) The change in open-circuit voltage losses ΔV_{OC} caused by parasitic light absorption (solid: $p_a = 0$; dashed: $p_a = 0.1$) as a function of the internal luminescence quantum efficiency Q_i^{lum} is shown for geometric concentrators ($p_e = 0.5$; $c_{geo} = 1, c_{ang} = 1$), angular restriction ($p_e = 0.005$; $c_{geo} = 1, c_{ang} = 100$), and the fluorescent concentrator ($p_e = 0.05$; $fc\ c_{geo} = 10$). The dashed lines correspond to the influence of parasitic light absorption with $p_a = 0.1$.

of $kT \ln(c_{ang})$ than the reference value $V_{OC}^{rad,1}$. However, upon decreasing Q_i^{lum} , the curve rapidly approaches that of the nonconcentrating cell because of $c_{geo} = 1$. Finally, the fluorescent collector calculated with the help of Eq. (38) displays a radiative limit that corresponds to a concentration factor of 100. This is due to the assumption of a spectral filter that restricts the emitted radiation i_{rad}^{em*} to 1% of the emitted radiation i_{rad}^{em} of the solar cell [31,115]. Note that, for simplicity, the reduction of the solar radiation i_{sun}^* by the spectral filter and the consequent small reduction of V_{OC} have been neglected [i.e. we have assumed $\log(i_{sun}^*/i_{sun}) \approx 0$]. Upon increasing nonradiative recombination ($Q_i^{lum} \ll 1$), the curve increasingly follows the assumed geometrical concentration factor $c_{geo} = 10$. Thus, a fluorescent collector equipped with a spectral filter displays different concentration factors: Close to the radiative limit, the concentration factor is defined by the reduced emission ($i_{rad}^{em}/i_{rad}^{em*} = 100$), and with nonradiative recombination dominating, the concentration factor is defined by the reduction of photovoltaic area ($c_{geo} = 10$).

The open-circuit voltage losses ΔV_{OC}^{nonr} due to nonradiative recombination and parasitic light absorption are summarized by terms 3 and 4 in Eq. (26). These losses are seen in Fig. 3(a) as the difference of the curves to their respective values of V_{OC}^{rad} at $Q_i^{lum} = 1$. Figure 2(b) visualizes these differences

without offset. For the understanding of the curves, it is helpful to note that the emission probability p_e defined in Eq. (25) may equally be expressed by $p_e = i_{rad}^{em}/(i_{rad}^{vol} c_{ang})$. Because of the assumption $i_{rad}^{em}/i_{rad}^{vol} = 0.5$ for all curves, the losses for the normal solar cell and all geometrical concentrators correspond to the curve with $p_e = 0.5$, whereas for the case of angular restriction, we have $p_e = 0.005$, and for the fluorescent concentrator, $p_e = 0.05$. The dashed lines in Fig. 3(b) correspond to the influence of parasitic light absorption with $p_a = 0.1$, instead of $p_a = 0$ for the solid lines. The largest influence attributed to parasitic absorption is seen for $Q_i^{lum} = 1$. Here, the loss ΔV_{OC}^{nonr} is entirely due to term 3 in Eq. (26). With decreasing Q_i^{lum} , the dashed curves approach the corresponding solid lines, i.e. the influence of parasitic absorption becomes negligible when compared to nonradiative recombination in the bulk.

Up to this point, we have seen that the influence of nonradiative loss processes, i.e. nonradiative recombination and parasitic absorption of solar cells embedded in different optical systems is well described by the present approach. However, the contributions of different entropic loss processes in Eq. (26) turn out as not being independent of each other even when only tuning a bulk property as Q_i^{lum} . This difficulty becomes even more pronounced when comparing different light-trapping schemes directly because each of the terms in Eq. (26) contains a contribution of the optical properties. The following section will show how to deal with this challenge.

IV. INFLUENCE OF LIGHT TRAPPING ON THE OPEN-CIRCUIT VOLTAGE

A. Path-length distribution in geometrical optics

Light trapping aims at enhancing J_{SC} , which is eventually defined by the absorptance $A(E)$ as a property of the absorber material and the solar spectrum [see Eq. (13)]. A convenient way to describe the quality of light-trapping schemes in geometrical optics independently from material and spectral properties is the path length distribution $P(l)$ [100,101,116]. Usually, the distribution $P(l)$ is condensed to its expectation value $\langle l \rangle$, the average path length. The insufficiencies of $\langle l \rangle$ as a figure of merit for the quality of light trapping in solar cells were first established to the field by Luque and Minano [44].

In this section, we will demonstrate illustratively the limited validity of $\langle l \rangle$ as a criterion for light trapping and derive an improved figure of merit. For a known dependence of the absorption coefficient α of the photovoltaic absorber material on photon energy E , we have

$$A(\alpha) = \int_0^\infty [1 - \exp(-\alpha l)] P(l) dl = 1 - N(\alpha), \quad (39)$$

where we have defined the nonabsorptance $N = 1 - A$. This quantity is defined by the Laplace transform of the path length distribution $P(l)$ via

$$N(\alpha) = \int_0^\infty P(l) \exp(-\alpha l) dl. \quad (40)$$

Note that, in the following, we assume for simplicity that there is neither direct reflection at the surface of the device nor parasitic absorption within the device such that N can be looked at as the portion of light that is reflected after at

least one passage through the device. This implies $P(l) = 0$ for $l < 2w$ and $N(\alpha) \rightarrow 0$ for $\alpha \rightarrow \infty$. Making use of the derivative theorem for the Laplace transform of Eq. (39), we obtain

$$-\frac{dN}{d\alpha} = \int_0^\infty lP(l) \exp(-\alpha l) dl = \frac{dA}{d\alpha}. \quad (41)$$

Based on Eq. (41), we can rewrite $\langle l \rangle$ by

$$\langle l \rangle = \int_0^\infty lP(l) = \lim_{\alpha \rightarrow 0} \frac{dA}{d\alpha}. \quad (42)$$

Eventually, the average path length $\langle l \rangle$ is the synonym for the derivative of the absorptance at $\alpha \rightarrow 0$, i.e. in the dilute limit where we have a very small absorptance A anyway. Since light trapping is aiming at maximizing J_{SC} in Eq. (13), we are more interested in optimizing the spectral range of intermediate A . Thus, the Yablonovitch criterion, though representing a thermodynamically well-defined limit, is not very suitable as a figure of merit to judge the quality of a light-trapping scheme. Alternatively, we propose to use the integral theorem of the Laplace transform

$$\int_\alpha^\infty N(\alpha') d\alpha' = \int_0^\infty \frac{1}{l} P(l) \exp(-\alpha l) dl \quad (43)$$

to define an alternative figure of merit. In the limit $\alpha \rightarrow 0$, Eq. (43) reads

$$\left\langle \frac{1}{l} \right\rangle = \int_0^\infty \frac{1}{l} P(l) dl = \int_0^\infty N(\alpha') d\alpha'. \quad (44)$$

Thus, minimizing the expectation value $\langle 1/l \rangle$ minimizes the integral nonabsorptance N , likewise maximizing the integral absorptance A . As we will show in the following, an effective path defined by Eq. (44) offers a much more selective figure of merit.

B. Lambertian light trapping

The paramount reference example for light trapping is the Lambertian situation where the light at one or both of the surfaces is completely randomized. As we will see in the following, the Lambertian scheme is only one of an infinite number that fulfill the Yablonovitch criterion, but it does not represent a specific limit. Thermodynamics and optics allow for the better and for the worse. However, for a theoretical treatment, Lambertian light trapping is relatively easy to handle and therefore a convenient reference.

In the following, we compare a Lambertian scheme to what we denote as partial Lambertian light trapping. We assume a semiconductor slab of thickness w with a perfectly flat back surface as illustrated in Fig. 4(a). With a probability p_λ , the incoming light is scattered at the front surface into a Lambertian distribution whose angle distribution is given by

$$P_L(\theta) = 2 \sin(\theta) \cos(\theta). \quad (45)$$

With a probability $1 - p_\lambda$, the light is coupled into the absorber according to Snell's law. After a single pass through the device, the light encounters again either Lambertian scattering or a flat surface. In the first case, a portion $T = 1/n^2$ of the light is lost to the ambient, whereas the remainder is redistributed according to Eq. (45). The quantity n denotes

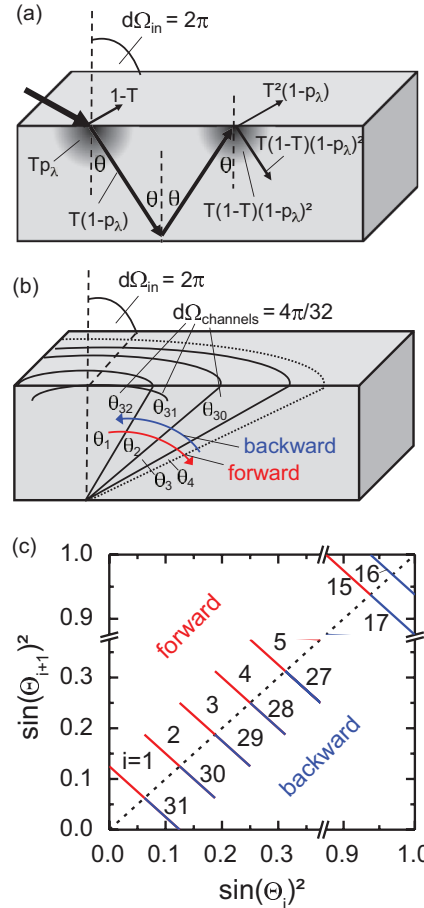


FIG. 4. (Color online) (a) Schematic illustration of the light scattering and light propagation for the partial Lambertian light-trapping scheme. (b) Schematic illustration of light propagation for the exemplary deterministic light-trapping scheme discussed in this contribution. The light cone is preserved during the 32 passes through the solar cell. The mapping rules for the redirection of the light at the front and rear interface are shown in (c).

the refractive index of the absorber material. In the second case, light is redirected into the absorber if its direction is given by an angle θ with $\sin^2(\theta) > 1/n^2$; otherwise, it is lost into the ambient. With this approach, we are able to describe a transition from perfect Lambertian light trapping with $p_\lambda = 1$ to the total absence of light trapping $p_\lambda = 0$. We use a simple Monte Carlo program for the calculations of absorptance and path length distribution. The results are compared to analytical expressions for perfect Lambertian light trapping with excellent agreement when using a number of rays $n_{\text{ray}} = 10^6$.

The model semiconductor used in the following calculations is defined by an absorption coefficient

$$\alpha = \alpha_0 \sqrt{\frac{E - E_g}{kT}}, \quad (46)$$

where α_0 is the absorption coefficient for a photon energy $E = E_g + kT$ with a band gap energy $E_g = 1.38$ eV. The semiconductor is assumed to have a refractive index $n = 4$.

The sun's spectrum is given by a black body radiation at $T_{\text{sun}} = 5800$ K.

Figure 4 shows (a) the calculated absorptance spectrum and (b) the corresponding path length distributions for probabilities p_λ between 1 and 0. The extreme value $p_\lambda = 0$ describes the case of no light scattering and coupling of incident light in the solar cell, and the extreme value $p_\lambda = 1$ describes the limit of complete Lambertian light trapping. Looking at the absorptance spectra of the quasi-Lambertian schemes with $1 > p_\lambda > 0$ in Fig. 5(a), we find that the slopes $dA/d\alpha$ at $\alpha = 0$ correspond to $4n^2$, i.e. the schemes fulfill the Yablonovitch criterion. This result, surprising at a first glance, follows from the fact that all these schemes couple all light directions inside the absorber to the outside world. This coupling becomes weaker with decreasing p_λ but is present as long as $p_\lambda > 0$. In other words, there are no perfect guided modes for $p_\lambda > 0$. Looking at the path length distributions $P(l)$ in Fig. 5(b), we see that decreasing p_λ leads to a strong increase for the probability of short paths, but at the same time also, very long path lengths become more probable because the weak coupling between inside directions and the outside world keeps some photons very long inside the absorber. In terms of the mean path length $\langle l \rangle$, both effects cancel out. Obviously, the weaker

coupling implies poorer light trapping and absorptance, which induces a decrease in J_{SC} according to Eq. (13). For the model semiconductor and a device thickness of $100 \mu\text{m}$, the J_{SC} decreases from 28.9 mA/cm^2 for the full Lambertian light trapping ($p_\lambda = 1$) to 16.1 mA/cm^2 for the partial Lambertian light trapping with $p_\lambda = 0.25$.

C. Deterministic versus random light trapping

Having learned that Lambertian light trapping is by far not the worst light-trapping scheme that fulfills the Yablonovitch criterion for vanishing absorption, we might wish to find out whether there are better ones. The key drawback of Lambertian light trapping and the associated random distribution of scattered light is the presence of very short paths within the distribution $P(l)$. Since the mean value of the length of light paths is fixed by the Yablonovitch criterion, narrowing the distribution would be the obvious choice as Luque and Minano showed in their contribution from 1991 [44]. If we would be able to confine to $P(l) = \delta(l - 4n^2w)$, the absorptance would read

$$A(\alpha) = 1 - \exp(-\alpha 4n^2w). \quad (47)$$

Of course, this optimum case is not realizable because coupling all directions inside the absorber to the outside world implies finite probabilities up to infinite path lengths. Thus, this optimum light trapping is rather an upper bound than an upper limit. However, as we will see in the following, it is possible to construct hypothetical light-trapping schemes in a gedankenexperiment that come very close to the optimum case. It shall be stressed that we do not provide any physical design for a light-trapping concept but rather theoretical considerations on the rules of light redirection in optimized light-trapping schemes that in principle obey all thermodynamic laws. In Fig. 4(b), such a light-trapping scheme is schematically illustrated. It will be called in the following the "deterministic light-trapping scheme". For this particular light-trapping scheme, incident light from the incoming solid angle $d\Omega_{\text{in}} = 2\pi$ at its incidence on the front interface is transmitted completely and is refracted into the solid angle cone $d\Omega_{\text{cone}} = 2\pi/n$ within the absorber layer volume (in this example, the refractive index is set to $n = 4$). As the solid angle cone exhibits rotational symmetry, it is well described by a single range of angles $d\theta_1$ [c.f. Fig. 3(b)]. Each time a light ray within the absorber volume impinges on the front or rear interface, it is redirected such that its angle θ_i increases for $0 < i \leq n$ and decreases for $n < i \leq 2n$. The detailed mapping rules are shown Fig. 4(c). As a consequence of the redirection, each light ray which impinges on the solar cell propagates $2n$ times from the front to the rear interface of the solar cell. Importantly, the solid angle cone $d\Omega_{\text{cone}} = 2\pi/n$ is preserved for all $2n$ redirections. In consequence, the full solid angle 4π in the absorber volume is accessed by the incident light impinging on the solar cell. In order to determine the absorptance and path length distribution for the deterministic light-trapping scheme, we use a simple Monte Carlo program. The results converged very well when using a number of rays $n_{\text{ray}} \geq 10^6$.

In Fig. 6(b), the path length distributions $P(l)$ of the deterministic light trapping is compared to Lambertian light trapping. It is shown that the deterministic light-trapping scheme exhibits a narrow path length distribution without

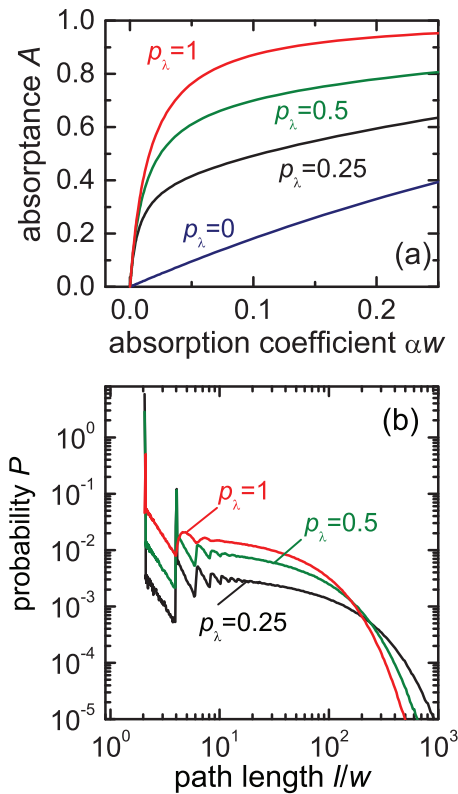


FIG. 5. (Color online) (a) The absorptance A of an ideal solar cell employing the partial Lambertian light-trapping scheme as a function of the thickness-corrected absorption coefficient (αw) with w being the thickness of the solar cell and α the energy dependent absorption coefficient. The probability p_λ , which denotes probability of incoming light being scattered at the front surface into Lambertian distribution, is varied from no light trapping ($p_\lambda = 0$) to Lambertian light trapping ($p_\lambda = 1$). (b) The path length distribution P as a function of the relative path length (l/w).

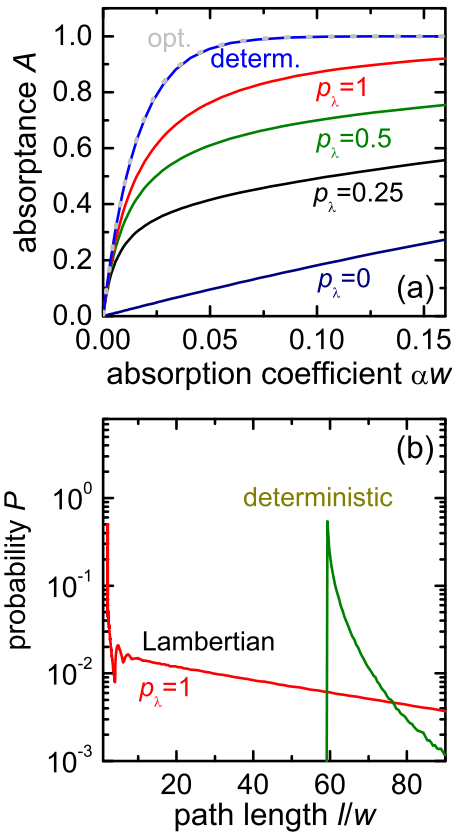


FIG. 6. (Color online) (a) The absorbance A of an ideal solar cell employing the deterministic light trapping, the partial Lambertian light-trapping scheme, as well as the optimal light trapping as an upper boundary are plotted as a function of the thickness-corrected absorption coefficient (αw) with w being the thickness of the solar cell and α the energy dependent absorption coefficient. (b) The path length distribution P is shown for the Lambertian light-trapping scheme and the deterministic light-trapping scheme as a function of the relative path length (l/w).

light paths of short lengths. In particular, the minimum path length of the deterministic light-trapping scheme is around 59 times the thickness of the solar cell if the refractive index is $n = 4$. In contrast, the Lambertian light-trapping scheme exhibits a broad distribution of paths lengths including very long paths but, most importantly, very short light paths down to twice the thickness of the solar cell. Since both light-trapping schemes fulfill the Yablonovitch criterion, their average light paths length is fixed at $4nw$ and, in turn, their absorbance intersects for vanishing absorption ($\alpha \rightarrow 0$). This aspect is presented in Fig. 6(a), which shows the absorbance of solar cell applying the Lambertian and deterministic light trapping as a function of the thickness corrected absorption (αw). Moreover, it is shown in Fig. 6(a) that, for nonvanishing absorption, the deterministic light trapping comes very close to the optimum case presented in Eq. (47). Hence, the presented deterministic light-trapping scheme outperforms the Lambertian light-trapping scheme for nonvanishing absorption in the solar cell. This aspect is attributed to the absence of short light paths for the deterministic light-trapping scheme. For nonvanishing absorption, due to the exponential correlation of absorbance and path lengths, the contribution to imperfect

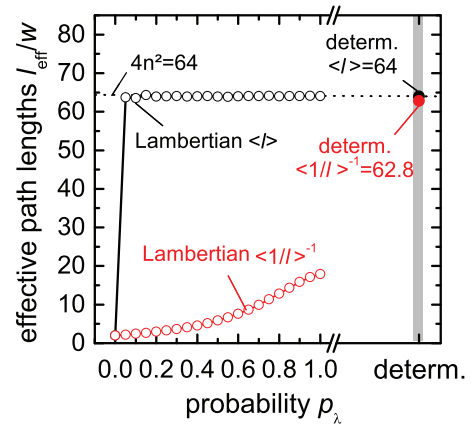


FIG. 7. (Color online) Effective path lengths $\langle l \rangle$ and $\langle 1/l \rangle^{-1}$ for partial Lambertian light trapping (open symbols), the deterministic light-trapping scheme (full symbols), and the value $4n^2$ (dashed line), which is the maximum value for $\langle l \rangle$ and an upper bound for $\langle 1/l \rangle^{-1}$.

absorbance in the solar cell increases stronger with decreasing path lengths than the length itself. As a consequence, short light paths must be avoided in order to exhibit good light trapping for nonvanishing absorption.

The relevance of avoiding short light paths in order to exhibit good light trapping in the case of nonvanishing absorption is reflected in the alternative figure of merit for light trapping, which we introduced in Sec. III A [see Eq. (44)]. It states that, by minimizing the expectation value $\langle 1/l \rangle$, the integral absorbance $\int A(\alpha) d\alpha$ is maximized. Figure 7 compares the effective path lengths $\langle l \rangle$ according to Eq. (42) and $\langle 1/l \rangle^{-1}$ according to Eq. (44) for partial Lambertian light-trapping schemes and the deterministic light-trapping scheme. The effective path length $\langle l \rangle = 64$ is the same for all curves belonging to (partial) Lambertian light trapping as soon as $p_\lambda > 0$, as well as for the deterministic case. In contrast, the alternative figure of merit $\langle 1/l \rangle^{-1}$ increases continuously with increasing p_λ . Furthermore, we have a marked difference between the completely randomized case ($p_\lambda = 1$) and the deterministic case. This is because the short light paths in the Lambertian case significantly contribute to increase $\langle 1/l \rangle$, i.e. to decrease $\langle 1/l \rangle^{-1}$. In contrast, deterministic light trapping avoids these paths totally.

It shall be noted that the presented deterministic light-trapping scheme is only one example for a light-trapping scheme which comes close to the optimal (upper bound) of light trapping. Several alternative rules for the redirection of the solid angle cone in the absorber volume of the solar cells can be imagined which induce a similarly high or even higher value of $\langle 1/l \rangle^{-1}$ where $\langle 1/l \rangle^{-1} = 4n^2$ is the upper bound only achieved by the physically impossible delta distribution $P(l) = \delta(l - 4n^2w)$. It shall also be noted that, strictly speaking, the illustrated design rules for the deterministic light trapping are only valid for even integer values of n^2 . Nevertheless, it is straightforward to design similar rules realizing almost comparable deterministic light-trapping schemes for arbitrary values of n .

Although the deterministic light-trapping scheme introduced in this section is a fully hypothetical concept which bears no physical structure for realization, it complies with the

laws of thermodynamics. Hence, it is useful for the discussion of the introduced figure of merit for light trapping as well as the discussion of general design principles such as the importance of avoiding shortest light paths for devices with intermediate absorptance.

D. Interplay between electrical properties, light trapping, and parasitic absorption

The interplay between electrical properties, namely V_{OC} and FF , and the light trapping as well as the parasitic absorption in the solar cell is illustrated for two exemplary cases. Of particular interest is the impact of the optical properties of the solar cell on the entropic losses of V_{OC} , which were subdivided in Eq. (26) into four terms. Optical Monte Carlo simulations of solar cells applying Lambertian or deterministic light-trapping schemes were conducted for the full spectral range in order to determine the absorptance A in the volume of the solar cell. In these simulations, parasitic absorption in the solar cells was considered as a fractional loss A_{BR} in the intensity of a light ray each time it impinges on the rear side of the solar cell. From the Monte Carlo simulations, the emission probability p_e , reabsorption probability p_r , and the parasitic absorption probability p_a of light emitted in the volume of the solar cells were derived. Knowing these quantities over the full spectral range, for a given internal luminescence quantum efficiency Q_i^{lum} and a given thickness w of the solar cell, V_{OC} can be calculated according to Eq. (26). Furthermore, since FF is well described by [117]

$$FF \approx \frac{qV_{OC}/kT_c - \ln \left\{ 0.72 + \frac{qV_{OC}}{kT_c} \right\}}{1 + \frac{qV_{OC}}{kT_c}}, \quad (48)$$

and J_{SC} is given by Eq. (13), we can calculate the energy conversion efficiency η of the solar cell for an ideality factor of unity.

In Fig. 8, J_{SC} , V_{OC} , and η of solar cells applying the deterministic light-trapping scheme are shown as a function of the effective thickness ($\alpha_0 w$). In the first series [Figs. 8(a)–8(c)], parasitic losses are not considered ($A_{BR} = 0$) and Q_i^{lum} is varied from 0.9 to 9×10^{-11} . Since J_{SC} depends ultimately on the absorptance A and is independent of Q_i^{lum} , it increases with increasing thickness of the solar cell until it saturates at the maximum J_{SC} . At maximum J_{SC} , all photons with energies above the band gap of the model semiconductor are absorbed. In contrast to J_{SC} , V_{OC} decreases for all effective thicknesses of the solar cell with increasing nonradiative recombination, i.e. decreasing Q_i^{lum} . This decrease is caused by nonradiative recombination in the volume of the solar cell which is an entropic loss process that reduces the V_{OC} [term 4 in Eq. (26)]. Furthermore, independent of Q_i^{lum} , V_{OC} also decreases with increasing thickness of the solar cell due to an decrease in the average generation rate over the volume and constant average recombination rate over the volume [118]. Also, with increasing thickness, the emission probability p_e decreases due to reabsorption, and in turn nonradiative recombination increases [see term 4 in Eq. (26)]. It is important to note that the emission probability p_e is a quantity related to the optical properties of the solar cell rather than a material-related quantity. Still, p_e strongly influences the entropic loss process associated with

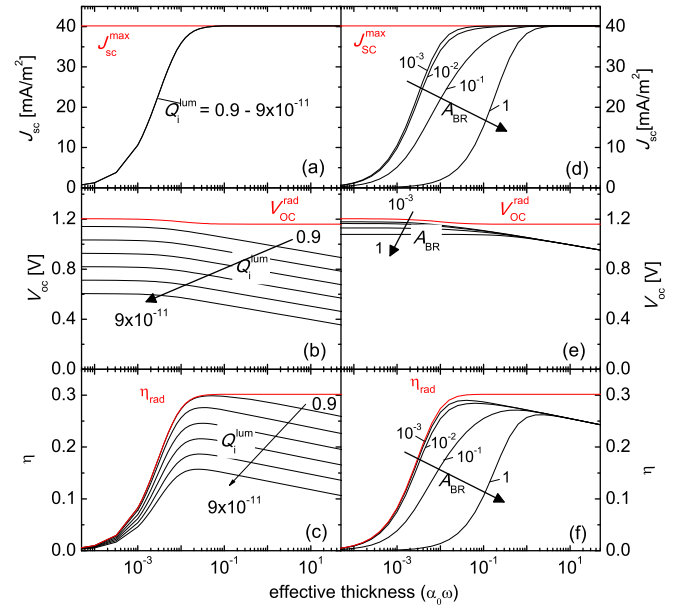


FIG. 8. (Color online) Short-circuit current density J_{SC} , open-circuit voltage V_{OC} , and energy conversion efficiency η of a solar cell applying the deterministic light-trapping scheme as a function of the effective thickness ($\alpha_0 w$). (a)–(c) The parasitic absorption is neglected $A_{BR} = 0$, and the internal luminescence quantum efficiency Q_i^{lum} is varied from 0.9 to 9×10^{-11} . (d)–(f) A_{BR} is varied from 10^{-3} to 10^0 , and the Q_i^{lum} is set to 0.5. For comparison, the reference quantities in the radiative limit (J_{SC}^{max} , V_{OC}^{rad} , η_{rad}) for zero parasitic absorptance and an infinitesimal thick solar cell are shown.

nonradiative recombination, which is truly material dependent. Hence, it is demonstrated that the entropic loss process in V_{OC} associated with nonradiative recombination depends strongly on the optical properties of the solar cell.

In the second series in Figs. 8(d)–8(f), the influence of parasitic losses is evaluated by varying the absorption at the back reflector ($A_{BR} = 10^{-3} - 1$) while keeping the amount of nonradiative recombination constant ($Q_i^{lum} = 0.5$). Obviously, for increasing parasitic absorption, J_{SC} of thin solar cells which exhibit weak absorption of incident light decreases. In order to reach a high J_{SC} , the thickness corrected absorption coefficient of these solar cells needs to be increased such that incident light is absorbed before it reaches the back reflector. Aside of J_{SC} , also V_{OC} of thin solar cells decreases with increasing parasitic absorption. However, in this case, the entropic losses that reduce the V_{OC} depend on three of the entropic loss processes described in Eq. (26). With increasing parasitic absorption, the absorptance A in the volume of the solar cell decreases, the emission probability p_e decreases, and the parasitic absorption probability p_a increases. Thus, three of the entropic loss processes that reduce the V_{OC} are changed: (i) the entropic loss in V_{OC} associated with photon cooling, (ii) the entropic loss in V_{OC} associated with parasitic absorption, and (iii) the entropic loss in V_{OC} associated with nonradiative recombination. This result is of high relevance, since it points out the impact of absorption losses in solar cells, i.e. light management, on V_{OC} . This interrelation is intensively discussed and researched in recent literature [5,66,67,119,120]; however, a correct derivation and

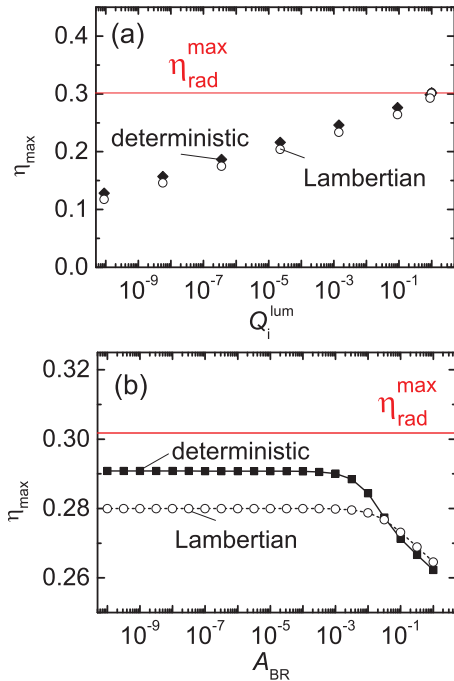


FIG. 9. (Color online) The maximum energy conversion efficiency η_{\max} for the deterministic light-trapping scheme (solid symbols) and the Lambertian light-trapping scheme (open symbols) as (a) a function of internal luminescence quantum efficiency Q_i^{lum} and (b) as a function of the parasitic absorption at the back reflector A_{BR} . For comparison, the maximum energy conversion efficiency radiative limit η_{rad}^{\max} is shown.

discrimination of all entropic loss terms reducing V_{OC} was missing, so far as we know.

While a discrimination of the contribution of these three terms will be discussed in the following section, at this stage, the strong influence of the optical properties of the solar cell on eventually all four entropic loss processes that reduce the V_{OC} shall be highlighted. For both series presented above, the J_{SC} increases, and V_{OC} decreases with increasing thickness of the solar cell. Thus, the energy conversion efficiency η exhibits a maximum conversion efficiency η_{\max} . In Fig. 9, the η_{\max} is shown for the deterministic light-trapping scheme and the Lambertian light-trapping scheme (a) as a function of Q_i^{lum} and (b) as a function of the parasitic absorption at the back reflector (A_{BR}). Independent on Q_i^{lum} and for parasitic absorption $A_{\text{BR}} < 0.05$, η_{\max} is larger for the deterministic light-trapping scheme than for the Lambertian light-trapping scheme. Eventually, this proves that the deterministic light-trapping scheme is also efficiency wise in most cases superior to the Lambertian light-trapping scheme. Only for very high parasitic absorption at the back reflector, due to the longer average first light pass through the solar cell, the η_{\max} of the Lambertian light-trapping scheme is larger when compared with the deterministic light-trapping scheme. However, if the mapping rules of the deterministic light-trapping scheme would be alternated such that incident light is redirected at the front interface into the solid angle cone of largest angles θ , the deterministic light would be superior to the Lambertian light trapping for any parasitic absorption.

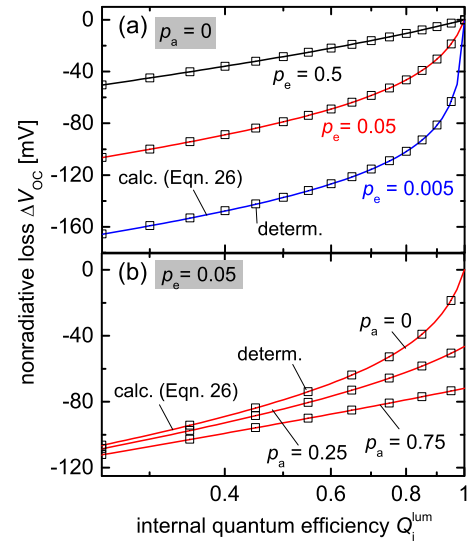


FIG. 10. (Color online) The open-circuit voltage losses ΔV_{OC}^r due to nonradiative recombination as a function of internal luminescence quantum efficiency Q_i^{lum} are calculated by term 4 in Eq. (26) (solid lines) and compared to the Monte Carlo simulations of deterministic light trapping (open symbols) for (a) a fixed $p_a = 0$ and $p_e = 0.005, 0.05$, and 0.5 and (b) a fixed $p_e = 0.05$ and $p_a = 0, 0.25$, and 0.75 .

E. Discrimination of entropic loss processes

Having studied the interrelation between the electrical properties, including V_{OC} , FF , and η , of solar cells and meaningful reference light-trapping schemes in the previous sections, these results will be set in the context of the general theory presented in Sec. III. In particular, the way light-trapping schemes influence the different types of entropic loss processes of V_{OC} , discriminated in Eq. (26), will be studied for the deterministic light-trapping scheme. First, in order to demonstrate the compatibility of the data derived from the Monte Carlo simulations and Eq. (26), we compare in Fig. 10 the nonradiative losses in V_{OC} as a function of Q_i^{lum} , calculated for a given p_a and p_e by term 4 in Eq. (26), to the nonradiative losses derived for the deterministic light trapping by Eq. (1). The good agreement for various absorption probabilities p_a and emission probabilities p_e shall be noted as a verification of the theory presented in Sec. III D by numerical experiments.

In detail, the discrimination of the entropic loss processes that reduce the V_{OC} for the reference case of no angular and no geometrical concentration ($c_{\text{ang}} = c_{\text{geo}} = 1$), geometrical concentration ($c_{\text{geo}} = 10$), and only angular concentration ($c_{\text{ang}} = 100$) is shown in Fig. 11. For comparison, in Fig. 11(a), the V_{OC} of these three cases are shown as a function of the luminescent quantum efficiency. In Figs. 11(b)–11(d), for the three light-trapping schemes, the contributions of entropic loss processes of V_{OC} are discriminated by considering the contributions of each of the four terms of Eq. (26) associated to four entropic loss processes. The term 1 considers the inherent entropic loss process of the device due to photon cooling which is independent of angular or geometrical concentration. The term 2 represents the entropic loss processes by étendue expansion; term 3 represents the entropic loss process by parasitic absorption of light and subsequent thermalization;

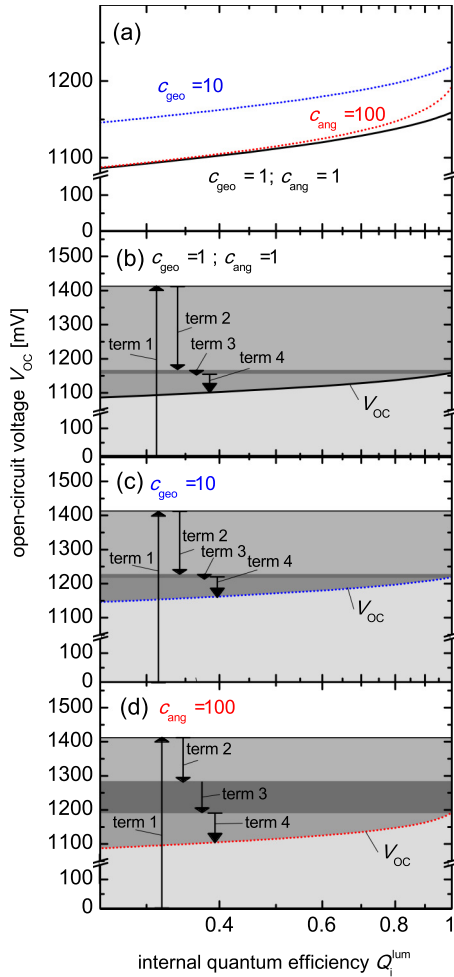


FIG. 11. (Color online) (a) Open-circuit voltage V_{OC} of solar cells employing the deterministic light trapping ($c_{ang} = c_{geo} = 1$), deterministic light trapping with geometrical concentration ($c_{geo} = 10$) and angular concentration ($c_{ang} = 100$) are shown as a function of the internal luminescence quantum efficiency Q_i^{lum} . The parasitic absorption at the back reflector A_{BR} is 2%. The discrimination of the four fundamental entropic loss processes decreasing the V_{OC} as described in Eq. (26) is shown for the three light-trapping schemes in (b)–(d), respectively.

and term 4 represents the entropic loss process by nonradiative recombination. For the reference case ($c_{ang} = c_{geo} = 1$), the change in V_{OC} with increasing Q_i^{lum} is caused by a reduction of the entropic losses due to nonradiative recombination (term 4). The losses attributed to étendue expansion (term 2) and parasitic losses (term 3) remain constant. For the case of geometrical concentration, the entropic losses caused

by nonradiative recombination and parasitic absorption are identical to the reference case. However, due to the geometrical concentration, the entropic losses by étendue expansion are decreased compared to the reference case, resulting in a positive contribution to the overall V_{OC} by term 2. Finally, for the case of angular restriction [see Fig. 11(c)], the entropic losses by photon cooling are identical to the reference case, but the entropic losses associated with étendue expansion are decreased since étendue of the emitted photons is decreased by c_{ang} . Furthermore, due to the angular concentration, a large fraction of the radiatively emitted photons is trapped in the solar cell which eventually increases the parasitic absorption loss compared to the case of no angular concentration. Finally, also the entropic losses due to nonradiative losses for ($Q_i^{lum} < 1$) are increased due to an increased nonradiative recombination of charge carriers which are generated by the reabsorption of trapped emitted photons due to angular concentration.

V. CONCLUSIONS

This paper presents a comprehensive theory of the thermodynamics of light management in solar cells considering explicitly imperfect light trapping, parasitic absorption, and nonradiative recombination losses. Our rigorous approach is compatible with the fundamental thermodynamic limits of light trapping (i.e. in the Yablonovitch limit) and of power conversion (i.e. in the Shockley-Queisser limit). It quantitatively describes entropic losses that reduce the open-circuit voltage and the energy conversion efficiency from the radiative limit towards realistic situations. The theory is applicable to a variety of solar cell devices like (i) solar cells with conventional light trapping, (ii) solar cells with geometric concentration of the incident light, (iii) solar cells with angular restriction of incoming and outgoing light, and (iv) luminescent concentrators. Our theory is applied in some detail to analyze conventional light trapping in nonconcentrating solar cells. Thereby, we introduce a new figure of merit for geometric light trapping, given by the mean inverse optical path length. The applicability of this figure of merit is demonstrated by the comparison of Lambertian light trapping and deterministic light trapping. We show that deterministic light-trapping concepts can outperform the Lambertian scheme by avoiding short light paths. Employing our theory to realistic solar cells, we demonstrate its particular strength to analyze the interplay between electrical properties and light management in solar cells as well as a unique way to discriminate between the different entropic losses in the open-circuit voltage for the various types of solar cell devices introduced.

- [1] R. B. Wehrspohn, A. Gombert, R. Carius, and U. Rau, *Phys. Stat. Sol. A* **205**, 2735 (2008).
- [2] H. A. Atwater and A. Polman, *Nat. Mater.* **9**, 205 (2010).
- [3] E. T. Yu and J. van de Lagemaat, *MRS Bull.* **36**, 424 (2011).
- [4] M. A. Green and S. Pillai, *Nat. Photon.* **6**, 130 (2012).

- [5] A. Polman and H. A. Atwater, *Nat. Mater.* **11**, 174 (2012).
- [6] C. Ulbrich, M. Peters, B. Blasi, T. Kirchartz, A. Gerber, and U. Rau, *Opt. Express* **18**, A133 (2010).
- [7] C. Ulbrich, S. Fahr, J. Upping, M. Peters, T. Kirchartz, C. Rockstuhl, R. Wehrspohn, A. Gombert, F. Lederer, and U. Rau, *Phys. Stat. Sol. A* **205**, 2831 (2008).

- [8] S. Fahr, C. Ulbrich, T. Kirchartz, U. Rau, C. Rockstuhl, and F. Lederer, *Opt. Express* **16**, 9332 (2008).
- [9] M. Peters, J. C. Goldschmidt, and B. Blasi, *J. Appl. Phys.* **110**, 043104 (2011).
- [10] J. B. Kim, P. Kim, N. C. Pegard, S. J. Oh, C. R. Kagan, J. W. Fleischer, H. A. Stone, and Y. L. Loo, *Nat. Photon.* **6**, 327 (2012).
- [11] B. Niesen, B. P. Rand, P. Van Dorpe, D. Cheyns, L. M. Tong, A. Dmitriev, and P. Heremans, *Adv. Energy Mater.* **3**, 145 (2013).
- [12] J. A. Schuller, E. S. Barnard, W. S. Cai, Y. C. Jun, J. S. White, and M. L. Brongersma, *Nat. Mater.* **9**, 193 (2010).
- [13] E. Stratakis and E. Kymakis, *Mater. Today* **16**, 133 (2013).
- [14] K. R. Catchpole and A. Polman, *Opt. Express* **16**, 21793 (2008).
- [15] K. R. Catchpole and A. Polman, *Appl. Phys. Lett.* **93**, 191113 (2008).
- [16] M. A. Green, *Prog. Photovolt.: Res. Applic.* **19**, 473 (2011).
- [17] Z. F. Yu, A. Raman, and S. H. Fan, *P. Natl. Acad. Sci. USA* **107**, 17491 (2010).
- [18] P. Bermel, C. Luo, L. Zeng, L. C. Kimerling, and J. D. Joannopoulos, *Opt. Express* **15**, 16986 (2007).
- [19] L. Zeng, P. Bermel, Y. Yi, B. A. Alamariu, K. A. Broderick, J. Liu, C. Hong, X. Duan, J. Joannopoulos, and L. C. Kimerling, *Appl. Phys. Lett.* **93**, 221105 (2008).
- [20] J. Upping, A. Bielawny, R. B. Wehrspohn, T. Beckers, R. Carius, U. Rau, S. Fahr, C. Rockstuhl, F. Lederer, M. Kroll, T. Pertsch, L. Steidl, and R. Zentel, *Adv. Mater.* **23**, 3896 (2011).
- [21] D. H. Ko, J. R. Tumbleston, L. Zhang, S. Williams, J. M. DeSimone, R. Lopez, and E. T. Samulski, *Nano Lett.* **9**, 2742 (2009).
- [22] J. R. Tumbleston, D. H. Ko, E. T. Samulski, and R. Lopez, *Opt. Express* **17**, 7670 (2009).
- [23] D. H. Ko, J. R. Tumbleston, A. Gadisa, M. Aryal, Y. C. Liu, R. Lopez, and E. T. Samulski, *J. Mater. Chem.* **21**, 16293 (2011).
- [24] Y. Yao, J. Yao, V. K. Narasimhan, Z. C. Ruan, C. Xie, S. H. Fan, and Y. Cui, *Nat. Commun.* **3**, 664 (2012).
- [25] J. Grandidier, D. M. Callahan, J. N. Munday, and H. A. Atwater, *Adv. Mater.* **23**, 1272 (2011).
- [26] P. Krogstrup, H. I. Jorgensen, M. Heiss, O. Demichel, J. V. Holm, M. Aagesen, J. Nygard, and A. F. I. Morral, *Nat. Photon.* **7**, 306 (2013).
- [27] M. D. Kelzenberg, S. W. Boettcher, J. A. Petykiewicz, D. B. Turner-Evans, M. C. Putnam, E. L. Warren, J. M. Spurgeon, R. M. Briggs, N. S. Lewis, and H. A. Atwater, *Nat. Mater.* **9**, 368 (2010).
- [28] E. Garnett and P. D. Yang, *Nano Lett.* **10**, 1082 (2010).
- [29] S. Brittman, H. W. Gao, E. C. Garnett, and P. D. Yang, *Nano Lett.* **11**, 5189 (2011).
- [30] J. Y. Tang, Z. Y. Huo, S. Brittman, H. W. Gao, and P. D. Yang, *Nat. Nano.* **6**, 568 (2011).
- [31] U. Rau, F. Einsele, and G. C. Glaeser, *Appl. Phys. Lett.* **87**, 171101 (2005).
- [32] N. C. Giebink, G. P. Wiederrecht, and M. R. Wasielewski, *Nat. Photon.* **5**, 694 (2011).
- [33] M. J. Currie, J. K. Mapel, T. D. Heidel, S. Goffri, and M. A. Baldo, *Science* **321**, 226 (2008).
- [34] J. C. Goldschmidt, M. Peters, A. Bosch, H. Helmers, F. Dimroth, S. W. Glunz, and G. Willeke, *Sol. Energy Mater. Sol. Cells* **93**, 176 (2009).
- [35] L. H. Slooff, E. E. Bende, A. R. Burgers, T. Budel, M. Pravettoni, R. P. Kenny, E. D. Dunlop, and A. Buchtemann, *Phys Status Solidi-R* **2**, 257 (2008).
- [36] W. G. J. H. van Sark, K. W. J. Barnham, L. H. Slooff, A. J. Chatten, A. Buchtemann, A. Meyer, S. J. McCormack, R. Koole, D. J. Farrell, R. Bose, E. E. Bende, A. R. Burgers, T. Budel, J. Quilitz, M. Kennedy, T. Meyer, C. D. M. Donega, A. Meijerink, and D. Vanmaekelbergh, *Opt. Express* **16**, 21773 (2008).
- [37] J. Bomm, A. Buchtemann, A. J. Chatten, R. Bose, D. J. Farrell, N. L. A. Chan, Y. Xiao, L. H. Slooff, T. Meyer, A. Meyer, W. G. J. H. van Sark, and R. Koole, *Sol. Energy Mater. Sol. Cells* **95**, 2087 (2011).
- [38] P. P. C. Verbunt, A. Kaiser, K. Hermans, C. W. M. Bastiaansen, D. J. Broer, and M. G. Debije, *Adv. Funct. Mater.* **19**, 2714 (2009).
- [39] D. Redfield, *Appl. Phys. Lett.* **25**, 647 (1974).
- [40] E. Yablonovitch, *J. Opt. Soc. Am.* **72**, 899 (1982).
- [41] E. Yablonovitch and G. D. Cody, *IEEE Trans. Elec. Dev.* **29**, 300 (1982).
- [42] T. Tiedje, E. Yablonovitch, G. D. Cody, and B. G. Brooks, *IEEE Trans. Elec. Dev.* **31**, 711 (1984).
- [43] M. A. Green, *Solar Cells, Operating Principles, Technology and System Applications* (University of New South Wales, Kensington, 1986), p. 79.
- [44] A. Luque and J. C. Minano, *Solar Cells* **31**, 237 (1991).
- [45] H. R. Stuart and D. G. Hall, *J. Opt. Soc. Am. A* **14**, 3001 (1997).
- [46] V. Badescu, *J. Phys. D: Appl. Phys.* **38**, 2166 (2005).
- [47] C. Rockstuhl, S. Fahr, and F. Lederer, *J. Appl. Phys.* **104**, 123102 (2008).
- [48] V. E. Ferry, L. A. Sweatlock, D. Pacifici, and H. A. Atwater, *Nano Lett.* **8**, 4391 (2008).
- [49] Z. F. Yu, A. Raman, and S. H. Fan, *Opt. Express* **18**, A366 (2010).
- [50] T. Markvart, *Appl. Phys. Lett.* **98**, 071107 (2011).
- [51] E. A. Schiff, *J. Appl. Phys.* **110**, 104501 (2011).
- [52] C. Battaglia, C. M. Hsu, K. Soderstrom, J. Escarre, F. J. Haug, M. Charriere, M. Boccard, M. Despeisse, D. T. L. Alexander, M. Cantoni, Y. Cui, and C. Ballif, *Acs Nano* **6**, 2790 (2012).
- [53] T. Markvart, L. Danos, L. P. Fang, T. Parel, and N. Soleimani, *Rsc Advances* **2**, 3173 (2012).
- [54] H. W. Deckman, C. R. Wronski, H. Witzke, and E. Yablonovitch, *Appl. Phys. Lett.* **42**, 968 (1983).
- [55] M. Peters, J. C. Goldschmidt, T. Kirchartz, and B. Blasi, *Sol. Energy Mater. Sol. Cells* **93**, 1721 (2009).
- [56] U. W. Paetzold, E. Moulin, B. E. Pieters, R. Carius, and U. Rau, *Opt. Express* **19**, A1219 (2011).
- [57] F. J. Beck, S. Mokkaapati, A. Polman, and K. R. Catchpole, *Appl. Phys. Lett.* **96**, 033113 (2010).
- [58] V. E. Ferry, M. A. Verschuuren, H. B. T. Li, E. Verhagen, R. J. Walters, R. E. I. Schropp, H. A. Atwater, and A. Polman, *Opt. Express* **18**, A237 (2010).
- [59] U. W. Paetzold, E. Moulin, D. Michaelis, W. Bottler, C. Wachter, V. Hagemann, M. Meier, R. Carius, and U. Rau, *Appl. Phys. Lett.* **99**, 181105 (2011).
- [60] A. J. Morfa, K. L. Rowlen, T. H. Reilly, M. J. Romero, and J. van de Lagemaat, *Appl. Phys. Lett.* **92**, 013504 (2008).

- [61] B. Wu, X. Wu, C. Guan, K. Fai Tai, E. K. L. Yeow, H. Jin Fan, N. Mathews, and T. C. Sum, *Nat. Commun.* **4**, 2004 (2013).
- [62] J. Wallentin, N. Anttu, D. Asoli, M. Huffman, I. Aberg, M. H. Magnusson, G. Siefer, P. Fuss-Kailuweit, F. Dimroth, B. Witzigmann, H. Q. Xu, L. Samuelson, K. Deppert, and M. T. Borgstrom, *Science* **339**, 1057 (2013).
- [63] B. Z. Tian, X. L. Zheng, T. J. Kempa, Y. Fang, N. F. Yu, G. H. Yu, J. L. Huang, and C. M. Lieber, *Nature* **449**, 885 (2007).
- [64] S. W. Boettcher, J. M. Spurgeon, M. C. Putnam, E. L. Warren, D. B. Turner-Evans, M. D. Kelzenberg, J. R. Maiolo, H. A. Atwater, and N. S. Lewis, *Science* **327**, 185 (2010).
- [65] M. A. Green, K. Emery, Y. Hishikawa, W. Warta, and E. D. Dunlop, *Prog. Photovolt. : Res. Applic.* **20**, 606 (2012).
- [66] O. D. Miller, E. Yablonovitch, and S. R. Kurtz, *IEEE J. Photov.* **2**, 303 (2012).
- [67] U. Rau and T. Kirchartz, *Nat. Mater.* **13**, 103 (2014).
- [68] H. A. Atwater and A. Polman, *Nat. Mater.* **13**, 104 (2014).
- [69] W. Shockley and H. J. Queisser, *J. Appl. Phys.* **32**, 510 (1961).
- [70] C. D. Mathers, *J. Appl. Phys.* **48**, 3181 (1977).
- [71] T. Tiedje, *Appl. Phys. Lett.* **40**, 627 (1982).
- [72] U. Rau and J. H. Werner, *Appl. Phys. Lett.* **84**, 3735 (2004).
- [73] T. Kirchartz, K. Taretto, and U. Rau, *J. Phys. Chem. C* **113**, 17958 (2009).
- [74] T. Kirchartz, J. Mattheis, and U. Rau, *Phys. Rev. B* **78**, 235320 (2008).
- [75] C. H. Henry, *J. Appl. Phys.* **51**, 4494 (1980).
- [76] G. L. Araujo and A. Marti, *Sol. Energy Mater. Sol. Cells* **33**, 213 (1994).
- [77] A. Luque and A. Marti, *Phys. Rev. Lett.* **78**, 5014 (1997).
- [78] J. H. Werner, S. Kolodinski, and H. J. Queisser, *Phys. Rev. Lett.* **72**, 3851 (1994).
- [79] M. C. Hanna and A. J. Nozik, *J. Appl. Phys.* **100**, 074510 (2006).
- [80] T. Kirchartz and U. Rau, *Thin Solid Films* **517**, 2438 (2009).
- [81] T. Markvart, *J. Appl. Phys.* **99**, 026101 (2006).
- [82] J. Mattheis, J. H. Werner, and U. Rau, *Phys. Rev. B* **77**, 085203 (2008).
- [83] R. T. Ross, *J. Chem. Phys.* **46**, 4590 (1967).
- [84] G. Smestad and H. Ries, *Sol. Energy Mater. Sol. Cells* **25**, 51 (1992).
- [85] U. Rau, *Phys. Rev. B* **76**, 085303 (2007).
- [86] G. Kirchhoff, *Annalen der Physik* **185**, 275 (1860).
- [87] M. Planck, *Vorlesungen ueber die Theorie der Waerme-strahlung* (Barth, Leipzig, 1906), p. 157.
- [88] P. Wurfel, *J. Phys. C: Solid State Phys.* **15**, 3967 (1982).
- [89] P. Wurfel, S. Finkbeiner, and E. Daub, *Appl. Phys. A: Mater. Sci. Process.* **60**, 67 (1995).
- [90] T. Kirchartz and U. Rau, *J. Appl. Phys.* **102**, 104510 (2007).
- [91] K. Vandewal, K. Tvingstedt, A. Gadisa, O. Ingnas, and J. V. Manca, *Nat. Mater.* **8**, 904 (2009).
- [92] T. Kirchartz, U. Rau, M. Kurth, J. Mattheis, and J. H. Werner, *Thin Solid Films* **515**, 6238 (2007).
- [93] S. Roensch, R. Hoheisel, F. Dimroth, and A. W. Bett, *Appl. Phys. Lett.* **98**, 251113 (2011).
- [94] T. Kirchartz, U. Rau, M. Hermle, A. W. Bett, A. Helbig, and J. H. Werner, *Appl. Phys. Lett.* **92**, 123502 (2008).
- [95] M. A. Green, *Prog. Photovolt.: Res. Applic.* **20**, 472 (2012).
- [96] W. Gong, M. A. Faist, N. J. Ekins-Daukes, Z. Xu, D. D. C. Bradley, J. Nelson, and T. Kirchartz, *Phys. Rev. B* **86**, 024201 (2012).
- [97] U. Hoyer, L. Pinna, T. Swonke, R. Auer, C. J. Brabec, T. Stubhan, and N. Li, *Adv. Energy Mater.* **1**, 1097 (2011).
- [98] T. C. M. Muller, B. E. Pieters, T. Kirchartz, and U. Rau, *Phys Status Solidi C* **9**, 1963 (2012).
- [99] M. A. Green, *Nano Lett.* **12**, 5985 (2012).
- [100] A. Luque in *Physical Limitations to Photovoltaic Energy Conversion*, edited by A. Luque and G. L. Araujo (Adam Hilger, Bristol, 1990).
- [101] J. C. Minano in *Physical Limitations to Photovoltaic Energy Conversion*, edited by A. Luque and G. L. Araujo (Adam Hilger, Bristol, 1990).
- [102] See Supplemental Material at <http://link.aps.org/supplemental/10.1103/PhysRevB.90.035211> for a derivation of Eq. (5).
- [103] M. A. Green, *IEEE Trans. Elec. Dev.* **31**, 671 (1984).
- [104] P. Campbell and M. A. Green, *IEEE Trans. Elec. Dev.* **33**, 234 (1986).
- [105] P. Würfel, *Physics of Solar Cells: From Basic Principles to Advanced Concepts* (Wiley-VCH, Weinheim, 2009).
- [106] M. A. Green, *Prog. Photovolt. : Res. Applic.* **9**, 257 (2001).
- [107] P. Baruch, *J. Appl. Phys.* **57**, 1347 (1985).
- [108] W. Ruppel and P. Wurfel, *IEEE Trans. Elec. Dev.* **27**, 877 (1980).
- [109] T. Markvart, *Phys. Stat. Sol. A* **205**, 2752 (2008).
- [110] L. C. Hirst and N. J. Ekins-Daukes, *Prog. Photovolt.: Res. Applic.* **19**, 286 (2011).
- [111] T. Markvart, *Appl. Phys. Lett.* **91**, 064102 (2007).
- [112] C. Donolato, *Appl. Phys. Lett.* **46**, 270 (1985).
- [113] W. van Roosbroeck and W. Shockley, *Phys. Rev.* **94**, 1558 (1954).
- [114] A. Goetzberger and W. Greubel, *Appl. Phys.* **14**, 123 (1977).
- [115] L. Proenneke, G. C. Glaeser, and U. Rau, *EPJ Photovoltaics* **3**, 30101 (2012).
- [116] R. Brendel, *Thin-Film Crystalline Silicon Solar Cells* (Wiley-VCH, Weinheim, 2003).
- [117] M. A. Green, *Solar Cells* **7**, 337 (1982).
- [118] R. Brendel and H. J. Queisser, *Sol. Energy Mater. Sol. Cells* **29**, 397 (1993).
- [119] M. A. Steiner, J. F. Geisz, I. Garcia, D. J. Friedman, A. Duda, W. J. Olavarria, M. Young, D. Kuciauskas, and S. R. Kurtz, *IEEE J. Photov.* **3**, 1437 (2013).
- [120] M. A. Steiner, J. F. Geisz, I. Garcia, D. J. Friedman, A. Duda, and S. R. Kurtz, *J. Appl. Phys.* **113**, 123109 (2013).